

FIM: A vertically flow-following, finite-volume icosahedral model

J.L. Lee¹, R. Bleck², A.E. MacDonald¹, J.-W. Bao¹,
S. Benjamin¹, J. Middlecoff³, N. Wang³, and J. Brown¹

¹NOAA/Earth System Research Laboratory (ESRL)

²Cooperative Institute for Research in Environmental Sciences (CIRES), CU

³Cooperative Institute for Research in the Atmosphere (CIRA), CSU

1. Introduction

Global Spectral models have gained almost universal acceptance in the last several decades. However, drawbacks of high-resolution spectral models in terms of operation counts and communication overheads on massive parallel processors have led, in recent years, to the development of new types of grid-point global models discretized on geodesic grids [see, e.g., Tomita et al. (2001)]. Among those, the icosahedral grid is attractive because it achieves quasi-uniform coverage of the globe with minimal regional variations in the shape of grid cells. If configured as a grid consisting of a large number of hexagonal cells (with 12 embedded pentagons), the icosahedral grid is particularly suitable for finite-volume numerics in which conventional finite-difference operators are replaced by numerically approximated line integrals along cell boundaries.

Williamson (1968) and Sadourny et al. (1968) were the first to solve shallow-water equations on icosahedral grids using finite-difference formulations. More recently, Colorado State University modelers (Heikes and Randall 1995; Ringler et al. 2000) developed an icosahedral-hexagonal shallow-water model (SWM) based on finite-volume numerics. The German Weather Service is currently using an icosahedral-hexagonal model for operational global weather prediction (Majewski et al. 2002). A Japanese group (Tomita et al. 2004) has developed a nonhydrostatic general circulation model (GCM) formulated on an icosahedral-hexagonal grid.

A flow-following finite-volume icosahedral model (FIM) is currently under development in the Global Systems Division of NOAA's Earth System Research Laboratory, with assistance from the Environmental Modeling Center (EMC) at the National Centers for Environmental Prediction (NCEP). The model combines a finite-volume icosahedral SWM solver with a "flow-following" vertical coordinate whose surfaces may deform freely according to air flow. Aloft, the flow-following coordinate is isentropic, which reduces spu-

rious nonphysical entropy sources in adiabatic flow (Johnson (1997)), while near the surface the coordinate surfaces are terrain-following. The coordinate is an improved version of the hybrid σ - θ coordinate successfully used in atmospheric and ocean models such as RUC (Rapid Update Cycle) and HYCOM (HYbrid Coordinate Ocean Model).

2. Model Descriptions

Denote the spatial coordinate by (x, y, s) where x, y are the common horizontal coordinates and s is an arbitrary but monotonic function of height, subject only to the requirement that the bottom and top of the model atmosphere are s surfaces. The physical dimensions of s are arbitrary; in fact, s can be chosen to be a continuous rendering of the coordinate surface index.

Let \mathbf{v} be the horizontal velocity vector; ∇_s the 2-D gradient operator at $s = \text{const}$; $\Pi = c_p(p/p_0)^{R/c_p}$ the Exner function; $\theta = c_p T/\Pi$ the potential temperature, $M = gz + \Pi\theta$ the Montgomery potential; ζ the vertical component of the velocity curl vector; $\dot{\theta}$ the net diabatic heating; and \mathbf{F} the sum of frictional forces. The set of dynamic equations solved in FIM can then be formulated as follows [see Kasahara (1974) and Bleck (1978a) for detailed derivations]

$$\frac{\partial \mathbf{v}}{\partial t} + (\zeta + f)\mathbf{k} \times \mathbf{v} + \left(\dot{s} \frac{\partial p}{\partial s} \right) \frac{\partial \mathbf{v}}{\partial p} + \nabla_s \left(M + \frac{\mathbf{v}^2}{2} \right) - \Pi \nabla_s \theta = \mathbf{F}$$

$$\frac{\partial}{\partial t} \left(\frac{\partial p}{\partial s} \right) + \nabla_s \cdot \left(\mathbf{v} \frac{\partial p}{\partial s} \right) + \frac{\partial}{\partial s} \left(\dot{s} \frac{\partial p}{\partial s} \right) = 0$$

$$\frac{\partial}{\partial t} \left(\theta \frac{\partial p}{\partial s} \right) + \nabla_s \cdot \left(\mathbf{v} \frac{\partial p}{\partial s} \theta \right) + \frac{\partial}{\partial s} \left(\dot{s} \frac{\partial p}{\partial s} \theta \right) = \dot{\theta} \frac{\partial p}{\partial s}$$

$$\frac{\partial M}{\partial \theta} = \Pi.$$

These equations are solved with finite-volume numerics which define model variables as mean quantities over each grid cell (van Leer (1977)). In the horizontal, equations are discretized on the icosahedral grid with conservative finite-volume operators including the curl, divergence, and gradient operators formulated as line integrals along the perimeter of each grid cell. On unstructured grids this approach ensures rigorous compliance with laws regarding global conservation of angular momentum, total mass, and pressure torques.

There are no explicit lateral mixing terms in the equations. The terms F in the first equation represents vertical momentum mixing, while the diabatic source term $\dot{\theta}(\partial p/\partial s)$ in the third equation above includes the effect of vertical mixing on potential temperature.

Discretization in the vertical is accomplished by integrating prognostic variables, as well as the equations governing their evolution, over individual layers bounded by s surfaces. Tendency terms in the prognostic equations are approximated by the explicit 3rd order Adam-Bashforth time differencing scheme.

FIM belongs to the class of *layer* models in which the vertical spacing of layer interfaces is variable in space and time, with interface movement controlled primarily by the convergence and divergence of lateral mass fluxes in each layer. To assure the numerical integrity of a layer model, mass fluxes must be constructed with strong emphasis on positive-definiteness and monotonicity. The scheme chosen for this purpose is the Flux-Corrected Transport (FCT) scheme (Zalesak 1979), extended to multiple time levels for use with the 3rd order Adam-Bashforth scheme. Physical parameterizations in FIM match those used operationally by the Global Forecast System (GFS) at NCEP.

3. Horizontal Grid

The icosahedral geodesic grid is generated from an icosahedron which has 12 vertices and 20 equilateral spherical triangles with 30 edges. Each edge is projected onto the sphere enclosing the icosahedron and hence becomes a segment of a great circle. The icosahedral grid provides quasi-uniform coverage of the sphere and allows hierarchical refinements of grid spacing. To increase grid resolution, each triangle is successively split into four smaller ones by bisecting each triangle edge. The corners of the new triangles are then projected onto the surface of the sphere enclosing the icosahedron. The more the triangles are split, the better the approximation of the polyhedron to the sphere. The total number of grid points, n , and the number of divisions, G , are connected through

$$n = 10 [(2^G)^2] + 2$$

The number of divisions G is referred to as the icosahedral grid level. For example, for the lowest grid level $G = 0$, the total number of grid points is $n = 12$, i.e., the original 12 icosahedral points. Fig. 1 shows the icosahedron with grid level G from 0 to 3. We have successfully tested FIM up to $G = 9$ where the average mesh size is 15 km.

All variables are carried at hexagon/pentagon centers, mimicking the Arakawa A grid. Interpolation to the cell perimeter for evaluating line integrals is 2nd order accurate.

4. Vertical Grid

The thickness of each coordinate layer in FIM is allowed to vary in space and time. Since the prognostic equations resemble the shallow-water equations, layer models are also referred to as stacked SWMs.

The hybrid grid in FIM resembles that of RUC (Bleck and Benjamin 1993; Benjamin et al. 2004). However, since the vertical staggering of variables in RUC is not conducive to formulating rigorously conservative finite-difference equations, FIM staggers variables in a manner analogous to the hybrid-isopycnic ocean model HYCOM (Bleck 2002). In other words, u, v, θ, q, M are treated as layer variables while $p, gz, \dot{s}\partial p/\partial s$ are carried on interfaces.

Layers in FIM conform to isentropic layers except in locations where the latter intersect the earth's surface. There, layers are locally redefined as terrain-following (σ coordinate) layers. An individual coordinate layer can be isentropic in one geographic region and terrain-following in another.

The hybridization concept employed here and in RUC differs from schemes developed elsewhere (Bleck 1978b; Konor and Arakawa 1997; Pierce et al. 1991; Zapotocny et al. 1994) in that it relies on local adjustment of the vertical grid spacing rather than on a fixed formula typically consisting of a weighted average of two or more "pure" coordinate choices. The present scheme adds one important element to the original Arbitrary Lagrangian-Eulerian (ALE) technique of Hirt et al. (1974): it provides a mechanism for keeping coordinate layers aligned with their designated *target* isentropes wherever possible. The original ALE scheme only concerned itself with the maintenance of nonzero grid spacing in Lagrangian coordinate simulations. While the flexibility of coordinate placement in ALE-type schemes is disconcerting to some users because grid point location in model space cannot be expressed in terms of a simple analytic formula, it allows the model designer to maximize the size of the isentropic domain. The reasoning underlying this assertion is that ALE sets the height above ground of the

Icosahedral Grid Generation

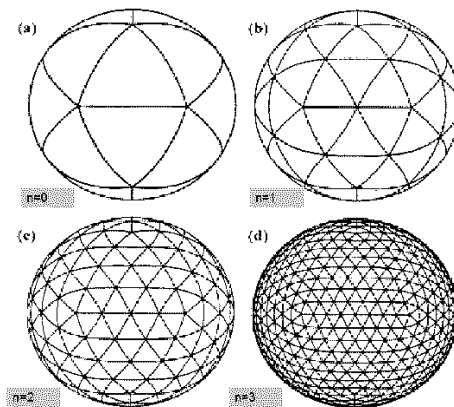


Figure 1: Icosahedral grid generation from grid level 0 to grid level 3

$\sigma - \theta$ coordinate transition in each grid column separately, i.e., unencumbered by global considerations. For additional details, see the draft FIM documentation at <http://fim.noaa.gov>.

5. Numerical Results

FIM has been evaluated in the 2-D context with the idealized cases of Williamson et al. (1992) for SWM flow on the sphere, and in the 3-D context with multi-month simulations of thermally forced mid latitude moist flow dominated by baroclinic instability over variable topography. Recently, we have started real data simulations. In this study, FIM was initialized with GFS initial condition for 00 UTC on October 9, 2003 on a G-5 grid which has an approximate mesh size of 250 km. In the vertical, there are 25 layers with target θ coordinate values covering the entire troposphere and lower stratosphere up to the model top at 20 mb.

Figures 2 and 3 show, respectively, FIM real-data initial conditions and 6-day model simulations. Fig. 2 shows the initial θ field superimposed by zonal wind isotachs in a vertical cross section along longitude 110°W . Model layer interfaces in Fig. 2 are depicted by solid contours with embedded squares. In the free atmosphere, θ is typically constant between two interfaces. The zonal wind cross section clearly shows mid latitude Jets near 200 mb and upper-level easterlies in the tropics. Note that layer interface spacing decreases near strengthening Jets, depicting increased stratification. This allows FIM to better resolve upper-level fronts and associated wind shears. Layer thickness near the ground, especially over mountains, is much smaller than in the free atmosphere. This, of course, is a matter of minimum layer thickness choice in the hybrid-isentropic “grid generator”. Fig. 3 is the same as Fig. 2 except that it shows 3- and 6-day fore-

casts. Fig. 3a, the 3-day forecast, shows that mid latitude Jets in both hemispheres are strengthening at that longitude compared to the initial condition. The isentropes underneath the northern hemispheric (NH) Jet are moving closer and increase their slope in response to the strengthening Jet. However, layer thickness remains finite and shows no small-scale noise, demonstrating the numerical resiliency of FIM. Fig. 3b, the 6-day forecast, shows that the strength of the NH Jet remains about the same, while the southern hemispheric (SH) Jet intensifies further during the last 3 days. Again, this is accompanied by reduced spacing and increased tilt of isentropes. These results, confirmed in runs at twice the vertical resolution (not shown here), indicate that the FCT scheme used in the mass continuity equation in FIM is able to handle tight interface spacing resulting from free interface movement without creating negative thickness values.

6. Summary and Outlook

A hydrostatic flow-following finite-volume icosahedral model, FIM, has been developed. The model has been evaluated with analytical test cases (not shown in this study) for two-dimensional flows as well as a real data case for three-dimensional flows. FIM is a global model free from pole problems typically seen in models based on spherical discretization. It makes use of positive-definite and monotonicity-preserving transport operators for mass and tracers, such as potential temperature and moisture, and uses curl, divergence, and gradient operators guaranteeing adherence to global conservation laws regarding angular momentum, mass, and pressure torques. In this study, we show that FIM is extraordinarily stable in real data simulations, requiring no explicit mixing/dissipation terms on time scales relevant to NWP. Results also confirm that FIM appears

to be free of potential numerical problems associated with flow-following coordinates, such as the dramatic thinning of coordinate layers near midlatitude Jets associated with upper-level frontogenesis. Results obtained at higher resolution, such as G7 (60 km mesh size) and 50 vertical layers, will be shown in the conference. The verification of FIM with reanalysis data in terms of vertical profiles and precipitation is currently underway. Plans for the future include a conversion of FIM's dynamic core to nonhydrostatic dynamics. More model information including technical details may be found at the FIM website at <http://fim.noaa.gov>.

References

- Benjamin, S., G. Grell, J. Brown, T. Smirnova, and R. Bleck, 2004: Mesoscale weather prediction with the ruc hybrid isentropic-terrain-following coordinate model. *Mon. Wea. Rev.*, **132**, 473–494.
- Bleck, R., 1978a: Finite difference equations in generalized vertical coordinates. part i: Total energy conservation. *Beitr. Phys. Atm.*, **51**, 360–372.
- 1978b: On the use of hybrid vertical coordinates in numerical weather prediction models. *Mon. Wea. Rev.*, **106**, 1233–1244.
- 2002: An oceanic general circulation model framed in hybrid isopycnic-cartesian coordinates. *Ocean Modelling*, **4**, 55–88.
- Bleck, R. and S. Benjamin, 1993: Regional weather prediction with a model combining terrain-following and isentropic coordinates. part 1: model description. *Mon. Wea. Rev.*, **121**, 1770–1785.
- Heikes, R. H. and D. A. Randall, 1995: Numerical integration of the shallow-water equations on a twisted icosahedral grid. i. basic design and results of tests. *Mon. Wea. Rev.*, **123**, 1862–...
- Hirt, C. W., A. A. Amsden, and J. L. Cook, 1974: An arbitrary langrangian-eulerian computing method for all flow speeds. *J. Comput. Phys.*, **14**, 227–253.
- Johnson, D. R., 1997: "general coldness of climate models" and the second law: Implications for modeling the earth system. *J. Climate*, **10**, 2826–2846.
- Kasahara, A., 1974: Various vertical coordinate systems used for numerical weather prediction. *Mon. Wea. Rev.*, **102**, 509–522.
- Konor, C. S. and A. Arakawa, 1997: Design of an atmospheric model based on a generalized vertical coordinate. *Mon. Wea. Rev.*, **125**, 1649–1673.
- Majewski, D., D. LierMann, P. Prohl, B. Ritter, M. Buchhold, T. Hanisch, G. Paul, and W. Wergen, 2002: The operational global icosahedral-hexagonal grid-point model gme: Description and high-resolution tests. *Mon. Wea. Rev.*, **130**, 319–338.
- Pierce, R., D. Johnson, F. Reames, T. Zapotocny, and B. Wolf, 1991: Numerical investigations with a hybrid isentropic-sigma model, part i: Normal mode characteristics. *J. Atmos. Sci.*, **48**, 2005–2024.
- Ringler, T. D., R. P. Heikes, and D. A. Randall, 2000: Modeling the atmospheric general circulation using a spherical geodesic grid: A new class of dynamical cores. *Mon. Wea. Rev.*, **128**, 2471–2490.
- Sadourny, R., A. Arakawa, and Y. Mintz, 1968: Integration of the non-divergent barotropic vorticity equation with an icosahedral-hexagonal grid for the sphere. *Mon. Wea. Rev.*, **96**, 351–356.
- Tomita, H., M. Satoh, and K. Goto, 2004: A new dynamical framework of global nonhydrostatic model using the icosahedral grid. *Fluid Dyn. Res.*, **34**, 357–400.
- Tomita, H., M. Tsugawa, M. Satoh, and K. Goto, 2001: Shallow water model on a modified icosahedral geodesic grid by using spring dynamics. *J. Comput. Phys.*, **174**, 579–613.
- van Leer, B., 1977: Towards the ultimate conservative difference scheme. iii. upstream-centered finite-difference schemes for ideal compressible flow. *J. Comput. Phys.*, **23**, 263–275.
- Williamson, D., 1968: Integration of the barotropic vorticity equation on a spherical geodesic grid. *Tellus*, **20**, 642–653.
- Williamson, D., J. B. Drake, J. J. Hack, R. Jakob, and P. N. Swarztrauber, 1992: A standard test set for numerical approximations to the shallow water equations in spherical geometry. *J. Comput. Phys.*, **102**, 221–224.
- Zalesak, S., 1979: Fully multidimensional flux-corrected transport algorithms for fluids. *J. Comput. Phys.*, **31**, 335–362.
- Zapotocny, T., D. Johnson, and F. Reames, 1994: Development and initial test of the university of wisconsin global isentropic-sigma model. *Mon. Wea. Rev.*, **122**, 2160–2178.

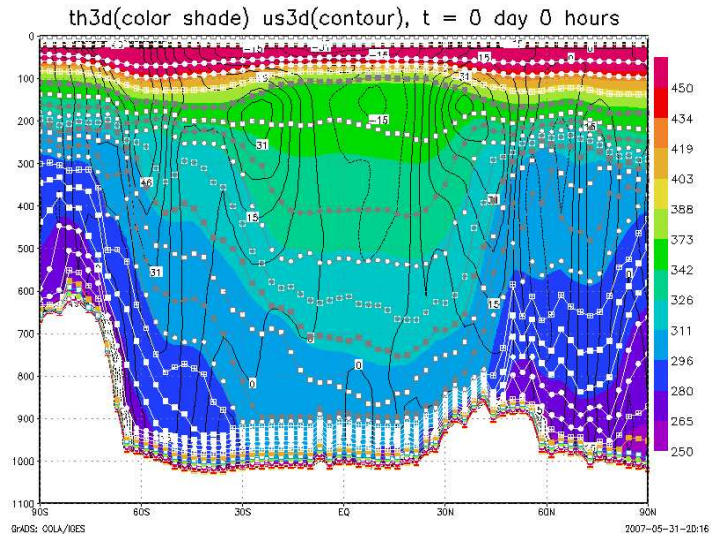


Figure 2: Initial condition for θ and u on the vertical cross section along the longitudinal at 110°

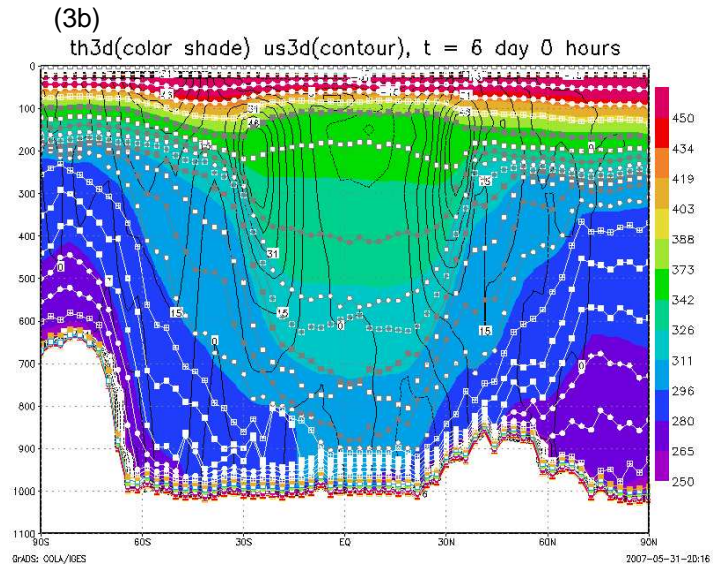
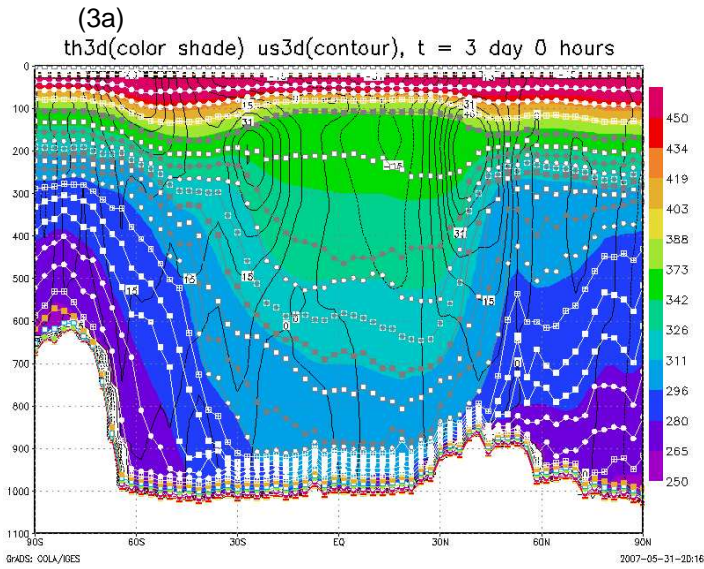


Figure 3: Same as Fig. 2 except for model 3-day forecast at (3a) and 6-day forecast at (3b)